



This is a repository copy of *Physiological Fluid Flow Moderates Fibroblast Responses to TGF- $\beta$ 1.*

White Rose Research Online URL for this paper:  
<http://eprints.whiterose.ac.uk/106886/>

Version: Accepted Version

---

**Article:**

Nithiananthan, S., Crawford, A., Cooper Knock, J. et al. (2 more authors) (2017)  
Physiological Fluid Flow Moderates Fibroblast Responses to TGF- $\beta$ 1. *Journal of Cellular Biochemistry*. ISSN 0730-2312

<https://doi.org/10.1002/jcb.25767>

---

This is the peer reviewed version of the following article: Nithiananthan, Sadhvi, et al. "Physiological Fluid Flow Moderates Fibroblast Responses to TGF- $\beta$ 1." *Journal of Cellular Biochemistry* (2016)., which has been published in final form at <http://doi.org/10.1002/jcb.25767>. This article may be used for non-commercial purposes in accordance with Wiley Terms and Conditions for Self-Archiving.

**Reuse**

Items deposited in White Rose Research Online are protected by copyright, with all rights reserved unless indicated otherwise. They may be downloaded and/or printed for private study, or other acts as permitted by national copyright laws. The publisher or other rights holders may allow further reproduction and re-use of the full text version. This is indicated by the licence information on the White Rose Research Online record for the item.

**Takedown**

If you consider content in White Rose Research Online to be in breach of UK law, please notify us by emailing [eprints@whiterose.ac.uk](mailto:eprints@whiterose.ac.uk) including the URL of the record and the reason for the withdrawal request.



[eprints@whiterose.ac.uk](mailto:eprints@whiterose.ac.uk)  
<https://eprints.whiterose.ac.uk/>

Research Article

## Physiological fluid flow moderates fibroblast responses to TGF- $\beta$ 1<sup>†</sup>

**Running title:** Fluid flow moderates fibroblast responses to TGF- $\beta$ 1.

**Sadhvi Nithiananthan<sup>1</sup>, Aileen Crawford<sup>2</sup> Johnathan Cooper Knock<sup>3</sup>, Daniel W. Lambert<sup>1</sup>, Simon A. Whawell<sup>1\*</sup>**

<sup>1</sup>Academic Unit of Oral & Maxillofacial Pathology, School of Clinical Dentistry, University of Sheffield, Sheffield UK.

<sup>2</sup>Academic Unit of Restorative Dentistry, School of Clinical Dentistry, University of Sheffield, Sheffield UK.

<sup>3</sup>Academic Neurology Unit, Department of Neuroscience, Sheffield Institute for Translational Neuroscience, University of Sheffield, Sheffield UK.

\*Corresponding author: Dr. Simon Whawell, Academic Unit of Oral & Maxillofacial Pathology, School of Clinical Dentistry, University of Sheffield, 19 Claremont Crescent Sheffield, S10 2TA. Tel: +44 114 271 7953 Email: s.whawell@sheffield.ac.uk

Abbreviations: transforming growth factor  $\beta$ 1 (TGF- $\beta$ 1), activin A (INHBA), follistatin (FST),  $\alpha$ -smooth muscle actin ( $\alpha$ -SMA), collagen IA1 (Col 1A1), caveolin 1A (CAV 1A), early endosomal antigen -1 (EEA-1), transforming growth factor  $\beta$  receptor type II (TGF $\beta$ RII), Gene Set Enrichment Analysis (GSEA), Gene Ontology term enrichment (GOTERM) and Kyoto Encyclopaedia of Genes and Genomes (KEGG).

Databases: <http://www.ebi.ac.uk/arrayexpress/arrays/E-MTAB-4905>.

**Keywords:** Fluid flow; TGF- $\beta$ 1;  $\alpha$ -SMA; activin A; follistatin; caveolin.

**Conflicts of Interest:** The authors confirm that there are no conflicts of interest for the study.

<sup>†</sup>This article has been accepted for publication and undergone full peer review but has not been through the copyediting, typesetting, pagination and proofreading process, which may lead to differences between this version and the Version of Record. Please cite this article as doi: [10.1002/jcb.25767]

**Received 2 August 2016; Revised 13 October 2016; Accepted 14 October 2016**

**Journal of Cellular Biochemistry**

**This article is protected by copyright. All rights reserved**

**DOI 10.1002/jcb.25767**

## Abstract

Fibroblasts are the major cellular component of connective tissue and experience mechanical perturbations due to matrix remodelling and interstitial fluid movement. Transforming growth factor  $\beta$ 1 (TGF- $\beta$ 1) can promote differentiation of fibroblasts *in vitro* to a contractile myofibroblastic phenotype characterised by the presence of  $\alpha$ -smooth muscle actin ( $\alpha$ -SMA) rich stress fibres. To study the role of mechanical stimulation in this process, we examined the response of primary human fibroblasts to physiological levels of fluid movement and its influence on fibroblast differentiation and responses to TGF- $\beta$ 1.

We report that in both oral and dermal fibroblasts, physiological levels of fluid flow induced widespread changes in gene expression compared to static cultures, including up-regulation of genes associated with TGF $\beta$  signalling and endocytosis. TGF- $\beta$ 1, activin A and markers of myofibroblast differentiation including  $\alpha$ -SMA and collagen IA1 were also increased by flow but surprisingly the combination of flow and exogenous TGF- $\beta$ 1 resulted in reduced differentiation. Our findings suggest this may result from enhanced internalisation of caveolin and TGF- $\beta$  receptor II.

These findings suggest that a) low levels of fluid flow induce myofibroblast differentiation and b) fluid flow antagonises the fibroblast response to pro-differentiation signals such as TGF- $\beta$ 1. We propose that this may be a novel mechanism by which mechanical forces buffer responses to chemical signals *in vivo*, maintaining a context-specific fibroblast phenotype.

This article is protected by copyright. All rights reserved

## Introduction

All living cells are constantly exposed to a number of physical forces. Repair and development of an organ or a tissue is governed by the integration of both physical forces and chemical signals (Mammoto and Ingber (2010). These physical forces comprise both endogenous forces such as cytoskeletal contractility and exogenous forces such as shear stress and interstitial fluid flow. Cells sense and respond to these different cues to maintain homeostasis. However, in pathological conditions such as fibrosis (Ban and Twigg, 2008) and cancer (Swartz and Lund, 2012) these adaptive mechanisms are disrupted.

The microenvironments of growing tumours and healing wounds are known to be highly dynamic (Schultz et al., 2011, Wiig et al., 2010) but generally display increased mechanical stiffness (Handorf et al., 2015) due to accumulation and reorganisation of extracellular matrix (ECM) proteins and increased interstitial fluid flow (Jain et al., 2014). Fibroblasts are the main cellular component of connective tissue and secrete components of ECM such as collagen and matrix modifying proteases including matrix metalloproteases (MMPs). They can differentiate into myofibroblasts when stimulated by TGF- $\beta$ 1 and other pro-differentiation signals (Hinsley et al., 2012), a transition which is characterised by increased phosphorylation of SMAD3 (Kamoto et al., 2013), enhanced expression of  $\alpha$ -smooth muscle actin ( $\alpha$ -SMA) (Honda et al., 2010), collagen IA1 and other matrix proteins (Pan et al., 2013). Myofibroblasts develop  $\alpha$ -SMA-rich stress fibres that enable them to contract to promote wound closure and upon completion of healing, they undergo apoptosis. However, in pathological conditions such as cancer where there are high levels of interstitial fluid flow and angiogenesis (Thannickal et al., 2004), fibroblasts remain activated indefinitely and this is associated with poor prognosis (Vered et al., 2009).

As most studies on TGF- $\beta$ 1-induced fibroblast differentiation have been pursued in a static culture environment, it is highly likely that TGF- $\beta$ 1 stimulated fibroblasts may show variations in their phenotype in a physiologically relevant, dynamic environment in which cells experience both physical forces and chemical signals.

The aim of this study was to investigate the response of fibroblasts to mechanical forces and chemical signals in a physiologically relevant dynamic environment. We report that fluid flow confers an „activated“ phenotype to normal fibroblasts and this differentiation is reversed when flow is withdrawn, and reduced in the presence of exogenous TGF- $\beta$ 1. We reveal that increased levels of TGF- $\beta$ 1 and activin A may mediate this activation of fibroblasts by flow, and that an increase in endocytosis including internalisation of TGF-  $\beta$ RII could explain the reduced response to TGF- $\beta$ 1 under flow. Our results provide the first evidence of fluid flow mediated “tensional homeostasis” that buffers the fibroblast phenotype in response to pro-differentiation signals such as TGF- $\beta$ 1 and mechanical forces experienced *in vivo*.

## Results

### Dermal fibroblasts show variations in gene expression when subjected to fluid flow

In order to identify fluid flow induced changes in gene expression profile of fibroblasts, we performed microarray analysis of transcript levels in dermal fibroblasts subjected to physiological rates of fluid flow (75 and 150  $\mu$ l/min) (A.Ahluwalia 2011, Sbrana and Ahluwalia, 2012, Vinci et al., 2010b) using the experimental set up illustrated in Figure 1a. Using this approach, we identified 2944 transcripts differentially expressed between dermal fibroblasts in static and flow conditions ( $p < 0.05$ ) at both flow rates (75 and 150  $\mu$ l/min) (Fig. 1b). The Volcano plot of the top 100 genes displaying variations in their expression under fluid flow (150  $\mu$ l/min) compared to static (Fig 1c). Principal Component Analysis (PCA) of the 2944 genes altered in dermal fibroblasts subjected to flow treatment (75 and 150  $\mu$ l/min) shows that the first principal component containing the majority of variability in these genes clearly separates the samples exposed to static conditions from the samples exposed to fluid flow (75 and 150  $\mu$ l/min) (Fig.1d). In order to further characterise the effects of fluid flow on fibroblasts the transcripts altered under flow (75 and 150  $\mu$ l/min) were examined for functional enrichment. The KEGG pathways which were most highly changed under flow were the TGF-  $\beta$  signalling pathway and genes associated with clathrin and caveolin-mediated endocytosis. Figure 1e and 1f show the top 20 flow altered genes ( $p < 0.01$ ) functionally associated with endocytosis and the TGF- $\beta$  pathway respectively.

## **Expression of $\alpha$ -SMA and collagen IA1 in dermal and oral fibroblasts is regulated by fluid flow.**

Given that genes associated with TGF- $\beta$  signalling were altered under fluid flow (75 and 150  $\mu$ l/min), in order to further characterise the effects of fluid flow on fibroblasts we studied gene expression changes in myofibroblast associated markers such as  $\alpha$ -SMA (Fig. 2a, b) and Col IA1 (Fig. 2c, d) in dermal and oral fibroblasts, subjected to fluid flow. TGF- $\beta$ 1 stimulated cells treated in static cultures were used as positive controls for myofibroblast differentiation. As previously reported (Hinsley et al., 2012), we observed that TGF- $\beta$ 1 stimulation increased the levels of  $\alpha$ -SMA and Col IA1 expression in dermal and oral fibroblasts in static conditions (Fig 2a,b). Fluid flow (150  $\mu$ l/min) increased  $\alpha$ -SMA gene expression by 1.9 fold in dermal and 3.9 fold in oral fibroblasts. Under the influence of fluid flow, Col IA1 gene expression increased by 3.4 fold in dermal and 1.5 fold in oral fibroblasts (Fig 2c, d). However, when TGF- $\beta$ 1 stimulated fibroblasts were treated by fluid flow (150  $\mu$ l/min),  $\alpha$ -SMA gene expression decreased by 1.1 fold in dermal and 3.4 fold in oral fibroblasts in comparison to those subjected to fluid flow treatment in the absence of TGF- $\beta$ 1 (Fig 2a, b). Similarly, Col IA1 gene expression also decreased by 2.3 fold in dermal fibroblasts and 0.9 fold in oral fibroblasts stimulated by TGF- $\beta$ 1 under conditions of fluid flow compared to fibroblasts subjected to fluid flow only (Fig 2c, d).

Dermal fibroblasts treated with fluid flow (150  $\mu$ l/min) revealed intense staining of  $\alpha$ -SMA rich stress fibres whereas TGF- $\beta$ 1 supplemented and flow treated fibroblasts show very little  $\alpha$ -SMA staining (Fig. 2e). Notably, these immunofluorescence studies on  $\alpha$ -SMA expression are concordant with the results from gene expression analysis. However, when dermal fibroblast subjected to fluid flow (150  $\mu$ l/min) for 24h. were allowed to rest in static conditions for 24h., the intensity of  $\alpha$ -SMA staining decreased (Fig.2f).

To study the functional role of TGF- $\beta$  pathway in fluid flow induced fibroblast activation by treating dermal fibroblasts with fluid flow for 2h. TGF- $\beta$ 1 supplemented and flow treated fibroblasts were used as positive controls. Expression of phosphorylated SMAD3 was studied by immunofluorescence (Fig 2g). and by western blotting (Fig 2h). Immunofluorescence findings indicated that

phosphorylated SMAD3 protein translocated to the nucleus under fluid flow treatment as well as in TGF- $\beta$ 1 supplemented and flow treated fibroblasts. Concordantly, protein blot analysis of phosphorylated SMAD3 also showed increase in protein expression when fibroblasts were subjected to fluid flow.

#### **Cell associated and secreted TGF- $\beta$ 1 is enhanced under fluid flow.**

To assess effect of fluid flow on protein expression of TGF- $\beta$ 1, we extracted protein samples from both cellular lysate and conditioned medium of dermal fibroblasts subjected to flow (150 $\mu$ l/min) and static treatments. Secreted TGF- $\beta$ 1 in conditioned medium (Fig. 3a) and cell associated TGF- $\beta$ 1 (Fig. 3b) were elevated in comparison to static cultures with secreted TGF- $\beta$ 1 protein being significantly ( $p < 0.01$ ) higher under flow. Further analysis by immunofluorescence detection of TGF- $\beta$ 1 revealed more intense staining in the perinuclear region in fibroblasts subjected to flow (Fig.3d) compared to those in static culture (Fig. 3c).

#### **Fluid flow enhances internalisation of caveolin-1A and nuclear translocation of the TGF- $\beta$ receptor type 2.**

To explore whether the decrease in the activation response in TGF-  $\beta$ 1-stimulated fibroblasts subjected to fluid flow was mediated by changes in endocytosis (Chen, 2009), we studied the protein expression of caveolin-1A under flow, with and without cell permeabilization to detect both membrane bound and cytoplasmic protein expression. The results showed that fibroblasts in static culture conditions had intense staining for caveolin-1A on the cell surface (Fig. 4a) and low cytoplasmic expression (Fig. 4b). Cytoplasmic expression of caveolin 1A was increased in fibroblasts subjected to flow in both TGF-  $\beta$ 1 stimulated and unstimulated conditions suggesting that under the influence of fluid flow, membrane bound caveolin 1A was internalised into the cell.

Fibroblasts under flow were double immunolabelled to simultaneously detect early endosomal antigen-1, an endosomal marker, and transforming growth factor beta receptor 2 (TGF- $\beta$ RII), the major physiological receptor for TGF-  $\beta$ 1 (Heldin and Moustakas, 2016)(Fig. 5). Little expression of EEA-1 and TGF- $\beta$ RII was detected in

fibroblasts in basal static conditions. TGF- $\beta$ 1 stimulation in static culture resulted in enhanced expression of EEA-1 and fluid flow treatment triggered not only a similar increase in expression of EEA-1 but also promoted internalisation and nuclear translocation of TGF- $\beta$ RII. The combination of TGF- $\beta$ 1 stimulation and fluid flow also induced nuclear translocation of TGF- $\beta$ RII (Fig 5).

### **Activin A expression is modulated by fluid flow.**

Our microarray analysis revealed activin A is one of the top 20 genes associated with the TGF- $\beta$  pathway altered under fluid flow, suggesting that activin A may play a role in fluid flow-mediated fibroblast activation and buffering of responses to TGF- $\beta$ 1. In concordance with the microarray results, qPCR analysis revealed activin A transcript levels were increased by 2.5 fold in dermal fibroblasts subjected to fluid flow for 24 h (Fig. 6a). This was reduced by 0.8 fold in TGF- $\beta$ 1 stimulated fibroblasts subjected to fluid flow as compared to those under fluid flow only. Cell-associated (Fig. 6b) and secreted (Fig. 6c) and protein levels of activin A were measured by ELISA in cell lysates and conditioned medium after fluid flow stimulation of dermal fibroblasts in the presence and absence of TGF- $\beta$ 1. Results revealed that activin A was significantly ( $p < 0.01$ ) increased in the conditioned culture medium and in cell extracts of fibroblasts subjected to flow. TGF- $\beta$ 1 stimulated fibroblasts in static and fluid flow conditions also showed elevated levels of cell-associated, but not secreted, activin A.

To study whether activation of fibroblasts is regulated by activin A, dermal fibroblasts were treated with 1 ng/ml activin A and  $\alpha$ -SMA protein was detected by immunofluorescence. It was observed that activin A stimulation in static conditions increased expression of  $\alpha$ -SMA (Fig. 7a) to a similar level observed in fibroblasts stimulated with TGF- $\beta$ 1. When activin A stimulated fibroblasts were treated with 1 ng/ml Follistatin-288, an activin A antagonist, protein expression of  $\alpha$ -SMA decreased in comparison to cells treated with activin A alone. Image J based quantification of  $\alpha$ -SMA staining (Fig. 7b and 7c) revealed that treatment of TGF- $\beta$ 1-stimulated dermal fibroblasts with follistatin-288 in static conditions also significantly decreased the protein expression of  $\alpha$ -SMA ( $p < 0.0001$ ). These results indicate that

activin A contributes to fluid flow-mediated and TGF- $\beta$ 1 stimulated fibroblast activation.

## Discussion

To date, studies on fibroblast differentiation have largely been pursued in static conditions where cells are devoid of physical signals that resemble interstitial fluid flow *in vivo*. The highly dynamic environment in which fibroblasts reside and the effect of locally derived signals in this physiologically relevant dynamic environment have been somewhat neglected to date. We report here that pathways mediating fibroblast activation are regulated by physiologically relevant fluid flow conditions.

We used the Quasi-vivo flow perfusion bioreactor to mimic shear stresses experienced by cells at a tissue level (A.Ahluwalia 2011, Vinci et al., 2010a). Under physiological conditions mesenchymal stem cells experience shear stresses in the order of 0.01 Pa to 0.1 Pa (Shieh and Swartz, 2011). From previous studies on the prototype of QV500 bioreactor used in our study, we have estimated that wall shear stress experienced by cells at a fluid flow velocity of 150  $\mu$ l/min is  $3.61 \times 10^{-6}$  Pa (Mazzei et al., 2010). Flow rates (75 and 150  $\mu$ l/min) used in our study are lower than those used in another study (500  $\mu$ l/min) where effect of fluid flow on hepatocyte proliferation and growth was increased (Vinci et al., 2010a). From the body of literature on the Quasi vivo bioreactor, we concluded that it is likely that the flow rates used in our study are within the physiological range in which cells are exposed to *in vivo*.

Our findings strengthen previous work where it was observed that interstitial fluid flow can activate fibroblasts when subjected to fluid flow at rate of 120 $\mu$ l/min (Ng et al., 2005). Here we show that even such low levels of shear stresses can induce changes in the global gene expression profile in both dermal and oral fibroblasts and activate fibroblasts of both dermal and oral origin. This included up-regulation of a number of members of the TGF- $\beta$  family, a group of growth factors with key roles in regulating fibroblast phenotype. Microarray analysis of highly enriched genes sorted on the basis of statistical significance altered under fluid flow at both 75 & 150  $\mu$ l/min showed up-regulation of TGF- $\beta$  pathway modulators such as activin A, SMAD7, and down-regulation of pathway antagonists.

TGF- $\beta$ 1 stimulation increased expression of  $\alpha$ -SMA in fibroblasts in static conditions, in keeping with our previous findings (Hinsley et al., 2012). Notably, fluid flow up-regulated gene expression of  $\alpha$ -SMA and Col IA1 in fibroblasts of both dermal and oral origin, despite there being evidence that there are phenotypic differences between fibroblasts from these two anatomical sites (Glim et al., 2014). However, TGF- $\beta$ 1 stimulation under fluid flow antagonised this activation response in cells of both origin. It is possible that the exogenous TGF- $\beta$ 1 in addition to increased endogenous levels with flow results in supra-physiological amounts which may inhibit this response. The fluid flow induced changes in fibroblast phenotype were shown to be reversible.

In order to begin to examine the signalling mechanisms underlying these observations, SMAD3 phosphorylation was analysed. SMAD3 is a transcription factor, which remains localised to the cytoplasm in un-stimulated cells. Upon activation of TGF- $\beta$  receptors, SMAD 3 is phosphorylated by TGF $\beta$ R1, Alk4 and Alk5 (Wrighton et al., 2009) and translocates to the nucleus. Nuclear localization of phosphorylated SMAD3 in dermal fibroblasts subjected to TGF- $\beta$ 1 stimulation and fluid flow suggests activation of the TGF- $\beta$  pathway even within 2 h of flow treatment. It is likely that SMAD3 is phosphorylated transiently due to elevated levels of TGF- $\beta$ 1 in the circulating medium even within 2 h flow and is dephosphorylated with time due to caveolin mediated membrane trafficking of TGF- $\beta$ 1 bound receptor complex into the nucleus. Whilst we cannot rule out the involvement of other signalling pathways, our microarray data reveal downregulation in gene expression of other R-SMADs from BMP signalling including SMAD1 and SMAD5.

Studies have shown that fluid flow induces shear stresses in the proximal tubule (Raghavan and Weisz, 2015, Raghavan et al., 2014). Notably in our study, genes associated with endocytosis were modified by fluid flow in fibroblasts. In line with this, intense staining of caveolin 1A is observed in the cytoplasm of fibroblasts subjected to fluid flow in the presence and absence of TGF- $\beta$ 1 suggesting endocytosis contributes to this fluid flow induced mechano-response in fibroblasts .

In our efforts to identify the molecular mechanisms responsible for fibroblast differentiation under flow and the buffering of responses to TGF- $\beta$ 1, we observed that recombinant activin A (a gene upregulated by flow) can activate dermal fibroblasts and that this is inhibited by follistatin 288. Follistatin-288 attenuates TGF- $\beta$ 1 mediated fibroblast differentiation by inhibiting not only activin A but also myostatin (Rodino-Klapac et al., 2009) a downstream regulator of the TGF- $\beta$  pathway. Activin A was down-regulated in TGF- $\beta$ 1 stimulated fibroblasts subjected to fluid flow conditions, thus strengthening our hypothesis that fibroblast activation is mediated by activin A. Fumagalli et al. 2007 have shown that in tissue sections of hypertrophic scars, there were high numbers of  $\alpha$ -SMA(+) myofibroblasts which co-express activin A. Furthermore, treatment of fibroblasts with activin A induced Akt phosphorylation, promoted cell proliferation, and enhanced  $\alpha$ -SMA and type I collagen expression. Follistatin reduced proliferation and suppressed activin-induced collagen expression suggesting that inhibition of activin A can potentially attenuate  $\alpha$ -SMA expression (Fumagalli et al., 2007). Although cell associated activin A was high in fibroblasts treated with TGF- $\beta$ 1 and flow, the protein was not secreted into the culture medium suggesting that secretion of activin A is inhibited by TGF- $\beta$ 1 supplementation. It is possible that secreted activin A competitively binds to the TGF- $\beta$  receptor type II (Aykul and Martinez-Hackert, 2016) and undergoes endocytosis mediated proteolytic degradation.

Although our data confirms previous finding that interstitial fluid flow promotes fibroblast differentiation via TGF- $\beta$ 1 (Ng et al., 2005, Shieh et al., 2011) at a fluid flow rate of 120 $\mu$ l/min; we show here for the first time that the combined effect of fluid flow and TGF- $\beta$ 1 reverses this process. We provide evidence that this effect is associated with rapid nuclear localisation of TGF- $\beta$ RII, which could result in disruption of TGF- $\beta$  Receptor type II receptor-ligand complexes and degradation of receptors (Del Galdo et al., 2008).

Our findings demonstrate that fibroblast responses to pro-differentiation signals, such as TGF- $\beta$ 1, are regulated by physiologically relevant physical forces and this factor must be considered when designing in vitro studies. Reversal of this activated phenotype in dermal fibroblasts upon withdrawal of fluid flow reveals that fibroblast activation through this mechanism is transient, and possibly indicates a mechanism

to respond to dynamic changes in the mechanical environment *in vivo* to allow homeostasis in connective tissue. We conclude that fluid flow acts as a homeostatic regulator of fibroblast phenotype, moderating fibroblast responses through the TGF- $\beta$  pathway. Our data provide the first direct evidence of fluid flow-mediated buffering of responses to chemical stimuli in fibroblasts.

## **Materials and Methods**

**Reagents and antibodies:** All of the reagents used in this study were purchased from Sigma unless otherwise stated. The antibodies used are shown in Table 1.

## **Cell Culture**

Normal oral fibroblasts (NOF-320) were derived from ethically approved waste tissues produced during oral surgical procedures undertaken at the Charles Clifford Dental Hospital, Sheffield, UK. Normal human dermal fibroblasts (NHDFC) were purchased from Promocell. Fibroblasts from both sources were cultured in DMEM supplemented with 10% (v/v) foetal calf serum (FCS) and 1% penicillin/streptomycin. Oral fibroblasts were used from a single donor at passage numbers between 3 and 5 and experiments were repeated three times. This study was approved by the University of Sheffield Ethics committee. (Ethics Committee approval Ref: 07/H1309/105).

## **Experimental design using the Quasi Vivo bioreactor**

The Quasi-Vivo bioreactor (Kirkstall Limited, UK) is composed of chambers of polydimethyl-siloxane (PDMS), interconnected in a series (Fig. 1a). A pump circulated DMEM containing 0.5% FCS over fibroblast cultures in six chambers of the bioreactor. The cells were subjected to a flow rate of either 75  $\mu\text{L}/\text{min}$  or 150  $\mu\text{L}/\text{min}$  for 24 h. For experimentation, cells were seeded onto glass coverslips in 24-well plates and maintained at 37°C for 48h prior to transferring into flow chambers.

## **Microarray analysis**

The effect of fluid flow was studied by subjecting dermal fibroblasts to varying fluid flow rates in the bioreactor for 24h. RNA was obtained from dermal fibroblasts exposed to 75  $\mu\text{L}/\text{min}$  and 150  $\mu\text{L}/\text{min}$  flow rate and linear amplification of the RNA was performed using the GeneChip® 3' IVT Express Kit (Affymetrix) according to the manufacturer's guidelines. Briefly, 200 ng RNA was reverse transcribed using an

oligo (dT) primers and then converted to double-stranded cDNA containing a T7 polymerase promoter site. Linear amplification was driven by a T7 promoter for 16 hours at 40°C and generated labelled antisense (aRNA) using biotinylated dUTPs. 15µg of aRNA was fragmented in buffer containing Mg<sup>2+</sup>, at 94 °C for 30 minutes and analysed using an RNA 6000 Nano Chip on the 2100 Bioanalyzer (Agilent). Hybridisation was carried out using the GeneChip® Hybridization, Wash, and Stain Kit (Affymetrix). Briefly 12.5 µg of fragmented aRNA was added to the mastermix solution containing pre-labelled hybridization controls (bioB, bioC, bioD, and cre genes) and positive oligonucleotide B2 control (B2 oligo). After 16 hours hybridisation at 42°C with rotation at 60 rpm, the Affymetrix U133 Plus 2.0 GeneChips were washed and stained in a GeneChip Fluidics Station 450 (Affymetrix) according to the manufacturer's protocol. Scanning was carried out on a GeneChip Scanner 3000 7G (Affymetrix). The scanned image files (.CEL) were processed using the Expression Console software (Affymetrix) for quality control checks and to generate a robust multiarray average (RMA) normalised dataset of the signal intensity for each probeset. Differential gene expression was determined using the Qlucore Omics explorer ([www.qlucore.com](http://www.qlucore.com)). Functional enrichment within differentially expressed genes was determined using the DAVID functional Annotation tool.

### **Immunofluorescence staining**

α-SMA protein was detected in dermal fibroblasts subjected to a flow rate of 150µl/ min for 24 h. Cells were stimulated with 10ng/ml TGF-β1 (R&D systems) in both static and flow conditions. Cells were fixed in 100% methanol and permeabilised with 4 mM sodium deoxycholate. Non-specific binding was blocked with 2.5% bovine serum albumin (BSA) in PBS followed by incubation with FITC conjugated anti-alpha smooth muscle actin (α-SMA) antibody in blocking buffer for one hour at 37°C.

Fibroblasts treated with fluid flow at a rate of 150µl/ min for 24 h. were left in static conditions for a further 24h and stained for α-SMA protein as above.

Dermal fibroblasts subjected to a flow rate of 150 µl/ min for 2 h. were labelled for phospho- SMAD3, CAV-1A, EEA-1 and TGFβRII. Cells stimulated with 10 ng/ml TGF-β1 (R&D systems) were used in both static and flow conditions. Staining was performed by fixing cells in 4% paraformaldehyde, followed by cell permeabilization in 0.5% Triton-X 100. Non-specific protein binding was blocked with 1% BSA in PBS after which the cells were incubated with primary antibodies (Table 1). Cells were

then mounted in DAPI containing anti-fade reagent and viewed under a fluorescent microscope (Zeiss Axioplan2, Imaging with software proplus 7.0.1).

TGF- $\beta$ 1 protein expression was detected in dermal fibroblasts subjected a flow rate of 150  $\mu$ l/ min for 24 h., followed by immunofluorescence staining as described above.

### **Quantitative PCR analysis**

Total RNA (100ng) was used as a template for cDNA synthesis using the High-Capacity cDNA Reverse Transcription Kit (Applied Biosystems) according to the manufacturer's guidelines. The tubes were placed into a thermal cycler (DNA engine DYAD) at 25°C for 10 min, 37°C for 2 h, and 85 ° C for 5 min and then held in 4°C. 0.5  $\mu$ l of cDNA was added to qRT-PCR mastermix containing 1x SYBR green mixture (Applied Biosystems) with gene specific primers for  $\alpha$ -SMA, Collagen IA1, Activin A and CD109 (Table 2). Assays were performed in triplicate on a 7900HT Fast real time PCR machine (Applied Biosystems) SDS version 2.4. and RQ Manager Version 1.2.1(Applied Biosystems) was used to record the CT values as determined from the SDS manager software. The delta CT values with reference to endogenous controls (U6) were calculated manually.

### **Immunoblotting**

Protein samples were extracted in RIPA lysis buffer containing protease and phosphatase inhibitors (Roche) from dermal fibroblasts subjected to fluid flow at 150  $\mu$ l/ min for 2 h. Cells stimulated with 10 ng/ml TGF- $\beta$ 1 (R&D systems) were used in both static and flow conditions. The protein concentration of each sample was determined using the BCA Protein Assay Kit (Thermo Fisher Scientific). 20  $\mu$ g of total protein extract was reduced in Sample Reducing Agent (10x), loaded with LDS Sample loading buffer (4X) (Nupage) and electrophoresed in 12-15% (v/v) polyacrylamide gels along with EZ-Run<sup>TM</sup> Prestained Rec Protein Ladder (Fisher Bioreagents). Protein was transferred to a 0.2  $\mu$ m nitrocellulose membrane (ProTran, GE Healthcare) using Trans-Blot<sup>®</sup> Turbo<sup>™</sup> Transfer System (GE Healthcare). The membranes were blocked in 5% bovine serum albumin in 1X TBS containing 0.1% Tween-20 overnight at 4°C. Membranes were incubated with rabbit monoclonal anti-Smad3 phospho S423 + S425 antibody for 1 h at room temperature. Nitrocellulose membranes were washed three times in the TBS-Tween and then incubated with HRP conjugated anti-rabbit secondary antibody for 1 h at room temperature and washed three times in TBS-T. Protein bands were visualized using a

chemiluminescence detection kit (ECL Western Blotting Substrate, Pierce) and developed using XPosure film in an automatic processor. In order to determine loading efficiency, membranes were routinely stripped with Restore™ Western Blot Stripping Buffer (Thermo Scientific), blocked in TBS Tween for 1 h and reprobed with  $\beta$ -actin antibody for 1 h. Membranes were washed three times with TBS Tween and probed with HRP conjugated secondary antibody for 1 h. The membranes were visualised as described above.

### **Enzyme linked immunosorbent assay (ELISA)**

Conditioned medium from cells were concentrated 5 times using Amicon Ultra-15 Centrifugal Filter Units. Cellular lysate samples were obtained using RIPA lysis buffer containing protease inhibitors and the protein concentration was determined as above. Activin A and TGF- $\beta$ 1 concentration was determined using Activin A Quantikine ELISA Kit and TGF $\beta$ 1 Emax® ImmunoAssay System (Promega Corporation), respectively, according to manufacturer's instructions. Activin A and TGF-  $\beta$ 1 concentration was estimated using the absorbance values of the standard curve and interpolating the test sample absorbance values using Graphpad Prism 7.

### **Statistical analyses**

Statistical significance of data was tested using one way ANOVA with multiple comparisons" test using Graph pad Prism.

## **Acknowledgments**

The authors are thankful to Dr. Paul Heath, Sheffield Institute of Translational Neuroscience, University of Sheffield for his support with microarray based experimental procedures and guidance on data analysis. All authors acknowledge the support from Dr. Kelly Davidge and Dr. Malcolm Wilkinson at Kirkstall Ltd for technical help with the bioreactor used in this study. The authors thank Mrs Brenka McCabe and Mr. Jason Heath for their technical assistance. This study is supported by The University of Sheffield, Faculty of Medicine Dentistry & Health Industrial Knowledge Exchange Fund. Sadhvi Nithiananthan is supported by a School of Clinical Dentistry, University of Sheffield Scholarship.

## **Authors contributions**

SN contributed towards designing experiments, performing them, analysing the data, and writing the paper. AC contributed in planning the experiments and writing the paper. JCK contributed towards analysing microarray data and paper writing. DWL and SAW contributed towards experimental planning, analysing the data and writing the paper.

## References

1. Fibroblast *Genetics Home Reference* [Online].
2. A.AHLUWALIA , F. V., F.MONTEMURRO AND M.WILKINSON 2011. Hepatotoxicity of diclofenac in a Quasi-Vivo(TM) multicompartiment bioreactor. *Toxicology letters*, 205, 270.
3. AYKUL, S. & MARTINEZ-HACKERT, E. 2016. Transforming Growth Factor-beta Family Ligands Can Function as Antagonists by Competing for Type II Receptor Binding. *J Biol Chem*, 291, 10792-804.
4. BAN, C. R. & TWIGG, S. M. 2008. Fibrosis in diabetes complications: Pathogenic mechanisms and circulating and urinary markers. *Vasc Health Risk Manag*, 4, 575-96.
5. CHEN, Y. G. 2009. Endocytic regulation of TGF-beta signaling. *Cell Res*, 19, 58-70.
6. DEL GALDO, F., LISANTI, M. P. & JIMENEZ, S. A. 2008. Caveolin-1, transforming growth factor-beta receptor internalization, and the pathogenesis of systemic sclerosis. *Curr Opin Rheumatol*, 20, 713-9.
7. FUMAGALLI, M., MUSSO, T., VERMI, W., SCUTERA, S., DANIELE, R., ALOTTO, D., CAMBIERI, I., OSTORERO, A., GENTILI, F., CAPOSIO, P., ZUCCA, M., SOZZANI, S., STELLA, M. & CASTAGNOLI, C. 2007. Imbalance between activin A and follistatin drives postburn hypertrophic scar formation in human skin. *Exp Dermatol*, 16, 600-10.
8. GLIM, J. E., EVERTS, V., NIESSEN, F. B., ULRICH, M. M. & BEELEN, R. H. 2014. Extracellular matrix components of oral mucosa differ from skin and resemble that of foetal skin. *Arch Oral Biol*, 59, 1048-55.
9. HANDORF, A. M., ZHOU, Y., HALANSKI, M. A. & LI, W. J. 2015. Tissue Stiffness Dictates Development, Homeostasis, and Disease Progression. *Organogenesis*, 11, 1-15.
10. HELDIN, C. H. & MOUSTAKAS, A. 2016. Signaling Receptors for TGF-beta Family Members. *Cold Spring Harb Perspect Biol*, 8.
11. HINSLEY, E. E., KUMAR, S., HUNTER, K. D., WHAWELL, S. A. & LAMBERT, D. W. 2012. Endothelin-1 stimulates oral fibroblasts to promote oral cancer invasion. *Life Sci*, 91, 557-61.
12. HONDA, E., YOSHIDA, K. & MUNAKATA, H. 2010. Transforming growth factor-beta upregulates the expression of integrin and related proteins in MRC-5 human myofibroblasts. *Tohoku J Exp Med*, 220, 319-27.
13. JAIN, R. K., MARTIN, J. D. & STYLIANOPOULOS, T. 2014. The role of mechanical forces in tumor growth and therapy. *Annu Rev Biomed Eng*, 16, 321-46.
14. KAMATO, D., BURCH, M. L., PIVA, T. J., REZAEI, H. B., ROSTAM, M. A., XU, S., ZHENG, W., LITTLE, P. J. & OSMAN, N. 2013. Transforming growth factor-beta signalling: role and consequences of Smad linker region phosphorylation. *Cell Signal*, 25, 2017-24.
15. MAMMOTO, T. & INGBER, D. E. 2010. Mechanical control of tissue and organ development. *Development*, 137, 1407-20.
16. MAZZEI, D., GUZZARDI, M. A., GIUSTI, S. & AHLUWALIA, A. 2010. A low shear stress modular bioreactor for connected cell culture under high flow rates. *Biotechnol Bioeng*, 106, 127-37.

17. NG, C. P., HINZ, B. & SWARTZ, M. A. 2005. Interstitial fluid flow induces myofibroblast differentiation and collagen alignment in vitro. *Journal of Cell Science*, 118, 4731-4739.
18. PAN, X., CHEN, Z., HUANG, R., YAO, Y. & MA, G. 2013. Transforming growth factor beta1 induces the expression of collagen type I by DNA methylation in cardiac fibroblasts. *PLoS One*, 8, e60335.
19. RAGHAVAN, V., RBAIBI, Y., PASTOR-SOLER, N. M., CARATTINO, M. D. & WEISZ, O. A. 2014. Shear stress-dependent regulation of apical endocytosis in renal proximal tubule cells mediated by primary cilia. *Proceedings of the National Academy of Sciences of the United States of America*, 111, 8506-8511.
20. RAGHAVAN, V. & WEISZ, O. A. 2015. Flow stimulated endocytosis in the proximal tubule. *Current opinion in nephrology and hypertension*, 24, 359-365.
21. RODINO-KLAPAC, L. R., HAIDET, A. M., KOTA, J., HANDY, C., KASPAR, B. K. & MENDELL, J. R. 2009. INHIBITION OF MYOSTATIN WITH EMPHASIS ON FOLLISTATIN AS A THERAPY FOR MUSCLE DISEASE. *Muscle Nerve*, 39, 283-96.
22. SBRANA, T. & AHLUWALIA, A. 2012. Engineering Quasi-Vivo in vitro organ models. *Adv Exp Med Biol*, 745, 138-53.
23. SCHULTZ, G. S., DAVIDSON, J. M., KIRSNER, R. S., BORNSTEIN, P. & HERMAN, I. M. 2011. Dynamic Reciprocity in the Wound Microenvironment. *Wound Repair Regen*, 19, 134-48.
24. SHIEH, A. C., ROZANSKY, H. A., HINZ, B. & SWARTZ, M. A. 2011. Tumor cell invasion is promoted by interstitial flow-induced matrix priming by stromal fibroblasts. *Cancer Res*, 71, 790-800.
25. SHIEH, A. C. & SWARTZ, M. A. 2011. Regulation of tumor invasion by interstitial fluid flow. *Phys Biol*, 8, 015012.
26. SWARTZ, M. A. & LUND, A. W. 2012. Lymphatic and interstitial flow in the tumour microenvironment: linking mechanobiology with immunity. *Nat Rev Cancer*, 12, 210-219.
27. THANNICKAL, V. J., TOEWS, G. B., WHITE, E. S., LYNCH, J. P., 3RD & MARTINEZ, F. J. 2004. Mechanisms of pulmonary fibrosis. *Annu Rev Med*, 55, 395-417.
28. VERED, M., ALLON, I., BUCHNER, A. & DAYAN, D. 2009. Stromal Myofibroblasts Accompany Modifications in the Epithelial Phenotype of Tongue Dysplastic and Malignant Lesions. *Cancer Microenvironment*, 2, 49-57.
29. VINCI, B., CAVALLONE, D., VOZZI, G., MAZZEI, D., DOMENICI, C., BRUNETTO, M. & AHLUWALIA, A. 2010a. In vitro liver model using microfabricated scaffolds in a modular bioreactor. *Biotechnol J*, 5, 232-41.
30. VINCI, B., MURPHY, E., IORI, E., MARESCOTTI, M. C., AVOGARO, A. & AHLUWALIA, A. 2010b. Flow-regulated glucose and lipid metabolism in adipose tissue, endothelial cell and hepatocyte cultures in a modular bioreactor. *Biotechnol J*, 5, 618-26.
31. WIIG, H., TENSTAD, O., IVERSEN, P. O., KALLURI, R. & BJERKVIG, R. 2010. Interstitial fluid: the overlooked component of the tumor microenvironment? *Fibrogenesis Tissue Repair*, 3, 12.
32. WRIGHTON, K. H., LIN, X. & FENG, X. H. 2009. Phospho-control of TGF- $\beta$  superfamily signaling. *Cell Res*, 19, 8-20.

## List of Tables:

**Table 1: Antibodies used:**

Antigen	Manufacturer	Application
Monoclonal Anti-Actin, $\alpha$ -Smooth Muscle - FITC ( $\alpha$ SMA) antibody produced in mouse (clone 1A4, F3777)	Sigma-Aldrich	1:100 for IF
Rabbit polyclonal Anti-Caveolin-1 (ab 2910)	Abcam	1:100 for IF
Rabbit monoclonal Anti-Smad3 phospho S423 + S425 antibody (ab52903)	Abcam	1:100 for IF, 1:1000 for WB
Rabbit polyclonal Transforming Growth Factor Beta Receptor Type II (TGF $\beta$ RII: L-21: SC-220)	Santa Cruz Biotechnology	1:50 for IF
Mouse monoclonal Early Endosomal Antigen-1 (610456)	B.D Biosciences	1:100 for IF
Anti-rabbit HRP-linked Antibody (7074)	New England Biolabs	1:3000 for WB
Donkey anti- rabbit Alexa Flour CY3 conjugated secondary antibody	Molecular probes	1:200 for IF
Donkey anti- mouse Alexa Flour FITC conjugated antibody.	Molecular probes	1:200 for IF
Monoclonal Anti $\beta$ Actin produced in mouse (A1978)	Sigma	1:10,000 for WB
Anti-Mouse HRP conjugated secondary Antibody (7076)	Cell signalling	1:3000 for WB
TGF Beta 1 Antibody (aa22-50) LS-C161825	Lifespan Biosciences	1:50 for IF

IF: Immunofluorescence; WB: Western Blot

**Table 2: Primers used for RT-PCR:**

Gene	Forward	Reverse
$\alpha$ -SMA collagen IA1	5" GAAGAAGAGGACAGCACTG3" 5"GTGGCCATCCAGCTGACC 3"	5"TCCCATTCCCACCATCAA3" 5" AGTGGTAGGTGATGTTCTGGGAG 3"
U6 actin A CD109	5" CTCGCTTCGGCAGCACA 3" 5"CCCCTTTGCCAACCTCAAA 3" 5"AGCTGCTCAAGACAGCATCA3"	5' AACGCTTCACGAATTTGCGT 3" 5"CATGGACATGGGTCTCAGCTT 3" 5"TTGGGGTCTGATGGAAGAGT3"

## Figure Legends:

**Figure 1: Gene expression changes when dermal fibroblasts were subjected to fluid flow.** a) Schematic diagram of Quasi Vivo bioreactor flow set up with six chambers connected with a pump circulating the medium over cells. Red arrows indicate direction of fluid flow. b) Heat map of 2944 transcripts that were differentially expressed under different flow rates (0, 75 and 150  $\mu\text{l}/\text{min}$ ) (t-test, p-value<0.05). c) Volcano plot of the top 100 differentially expressed transcripts by p-value. d) Factorisation by principal components was performed for fibroblast expression of the 2944 transcripts which are altered under flow (75 and 150  $\mu\text{l}/\text{min}$ ). The fibroblasts are plotted on the first three principal components; fibroblasts exposed to 75 $\mu\text{L}/\text{min}$  are plotted in yellow, fibroblasts exposed to 150  $\mu\text{l}/\text{min}$  are plotted in cyan, and fibroblasts in static conditions are plotted in blue. e) Top 20 genes associated with endocytosis altered under fluid flow (150  $\mu\text{l}/\text{min}$ ) (p<0.01) and f) Top 20 genes associated with TGF- $\beta$  pathway altered under fluid flow (p<0.01).

**Figure 2: Expression of  $\alpha$ -SMA, Collagen IA1 and phospho-SMAD3 under flow (150  $\mu\text{L}/\text{min}$ ).** Expression of  $\alpha$ -SMA with fold change relative to endogenous control a) in Dermal (n=3) and b) Oral fibroblasts (n=3) (p < 0.05) subjected to flow. Expression of Collagen IA1 with fold change relative to endogenous control c) in Dermal (n=3) (p < 0.05) and d) Oral fibroblasts (n=3) (p < 0.05) subjected to flow. Error bars represent  $\pm\text{SEM}$ . e) Dermal Fibroblasts subjected to static conditions  $\pm\text{TGF-}\beta$ 1 flow  $\pm\text{TGF-}\beta$ 1 for 24h (n=3). f) Dermal Fibroblasts subjected to static conditions  $\pm\text{TGF-}\beta$ 1 flow  $\pm\text{TGF-}\beta$ 1 and subjected to recovery in static conditions for 24h (n=3), g) Dermal Fibroblasts subjected to flow for 2h. and stained with phospho-SMAD3, h) Expression of phospho-SMAD3 protein relative to  $\beta$ -actin expression in dermal fibroblasts. All images were captured at 1000X magnification using the same exposure time.

**Figure 3: Changes in expression of caveolin 1a in dermal fibroblasts subjected to fluid flow (150 $\mu\text{l}/\text{min}$ ) for 2h.** a) Cell surface protein expression of caveolin-1A (green) in unpermeabilised dermal fibroblasts and b) cytoplasmic expression of caveolin-1A protein in permeabilised fibroblasts.

**Figure 4: Expression of transforming growth factor  $\beta$  receptor type 2 and early endosomal antigen-1 in dermal fibroblasts subjected to flow (150  $\mu$ L/min) for 2 h.** Cells are stained with EEA-1 (green; 1), TGF- $\beta$ RII (red; 2), and DAPI (blue; 3) and merged images (red, blue, green; 4) in fibroblasts treated a) in static conditions b) static conditions stimulated with TGF- $\beta$ 1 c) fluid flow and d) fluid flow stimulated with TGF- $\beta$ 1. All images were captured at 100X magnification.

**Figure 5: Expression of transforming growth factor  $\beta$ 1 in dermal fibroblasts subjected to flow (150  $\mu$ L/min) for 24h.** a) Secreted TGF- $\beta$ 1 protein expression in dermal fibroblasts subjected to fluid flow at 150  $\mu$ L/min (n=3) (\* represents  $p < 0.05$ ), b) Protein expression of cellular TGF- $\beta$ 1 in dermal fibroblasts subjected to fluid flow at 150  $\mu$ L/min (n=2). Immunofluorescence detection of TGF- $\beta$ 1 in c) dermal fibroblasts treated in static conditions and d) dermal fibroblasts subjected to flow (n=3).

**Figure 6: Expression of activin A in dermal fibroblasts subjected to fluid flow (150  $\mu$ L/min) treatment for 24h.** a) Gene expression of activin A with fold change relative to endogenous control dermal fibroblasts subjected to flow (n=3) (\* represents  $p < 0.05$ ), b) Protein expression of cell associated activin A (n=3) (\*\*\*) represents  $p < 0.0001$ ) and c) Protein expression of secreted activin A in dermal fibroblasts subjected to fluid flow (n=3) (\*\*\*) represents  $p < 0.0001$ ).

**Figure 7: Protein expression of  $\alpha$ -SMA protein in dermal fibroblasts subjected to fluid flow (150  $\mu$ L/min), follistatin-288, TGF- $\beta$ 1 and activin A treatment for 24h.** a) Expression of  $\alpha$ -SMA protein in dermal fibroblasts subjected to fluid flow (150  $\mu$ L/min) for 24h (n=3) Top panel: TGF- $\beta$ 1 (10 ng/ml), activin A (1 ng/ml), fluid flow (150  $\mu$ L/min) and Bottom panel: Follistatin (1 ng/ml), TGF- $\beta$ 1 (10 ng/ml) treated with follistatin (1 ng/ml), activin A (1 ng/ml) treated with follistatin (1 ng/ml), Fluid flow (150  $\mu$ L/min) treated with follistatin (1ng/ml). b) Image J based quantification of  $\alpha$ -SMA protein in dermal fibroblasts subjected to fluid flow (150  $\mu$ L/min) for 24h (n=3), treated with minimal medium, TGF- $\beta$ 1 (10 ng/ml), follistatin (1 ng/ml), activin A (1 ng/ml), activin A (1 ng/ml) in combination with follistatin (1 ng/ml) and c) Image J based quantification of  $\alpha$ -SMA protein in dermal fibroblasts in dermal fibroblasts treated with TGF- $\beta$ 1 (10ng/ml), TGF- $\beta$ 1 (10 ng/ml) in combination with follistatin (1

ng/ml), fluid flow (150  $\mu$ l/min) in combination with follistatin (1 ng/ml). All images were captured at 1000 X magnification. Statistical bars represent p-value<0.0001, error bars represent  $\pm$  SEM.

**Figure 1:**

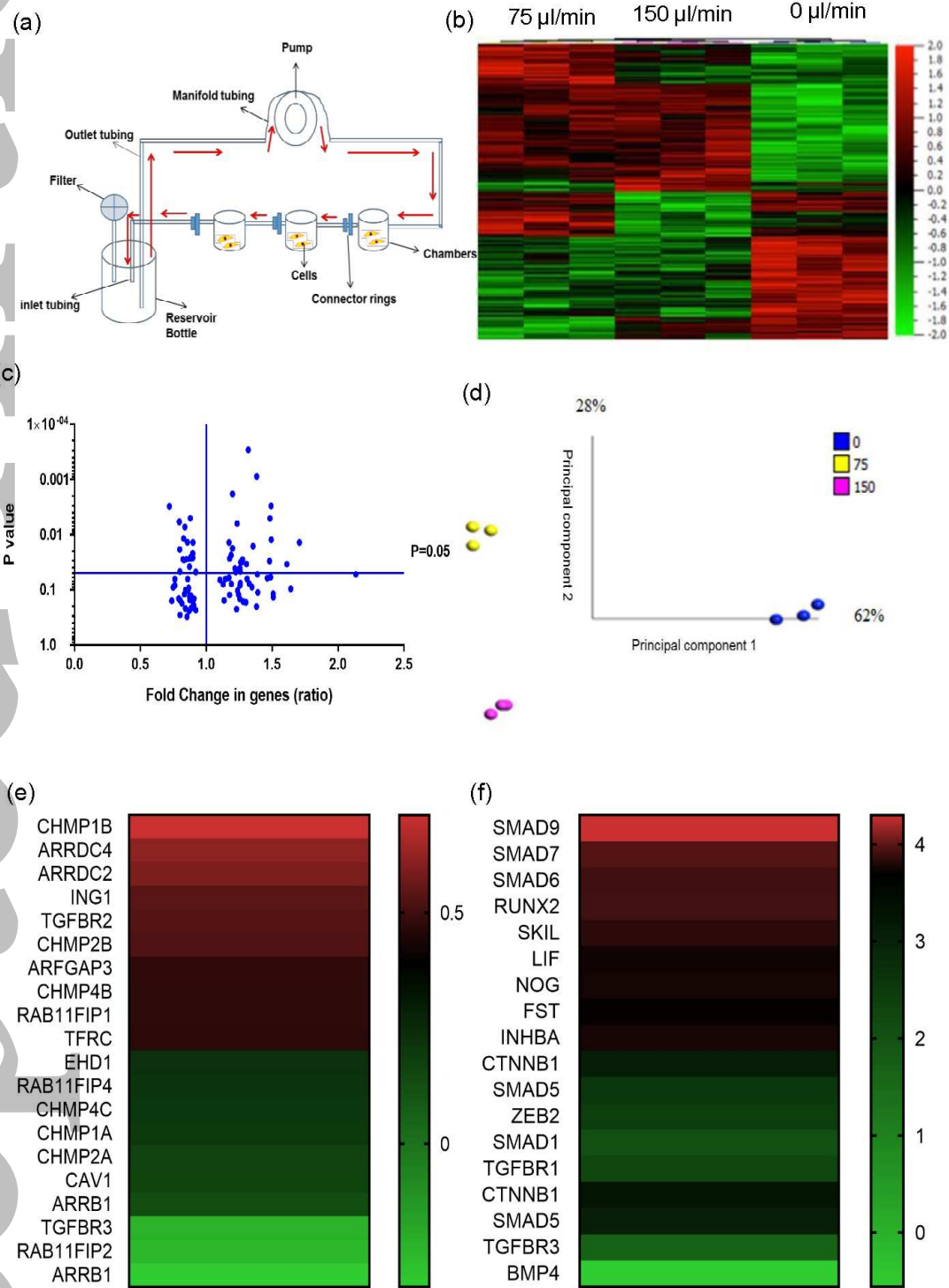


**Figure 2:**

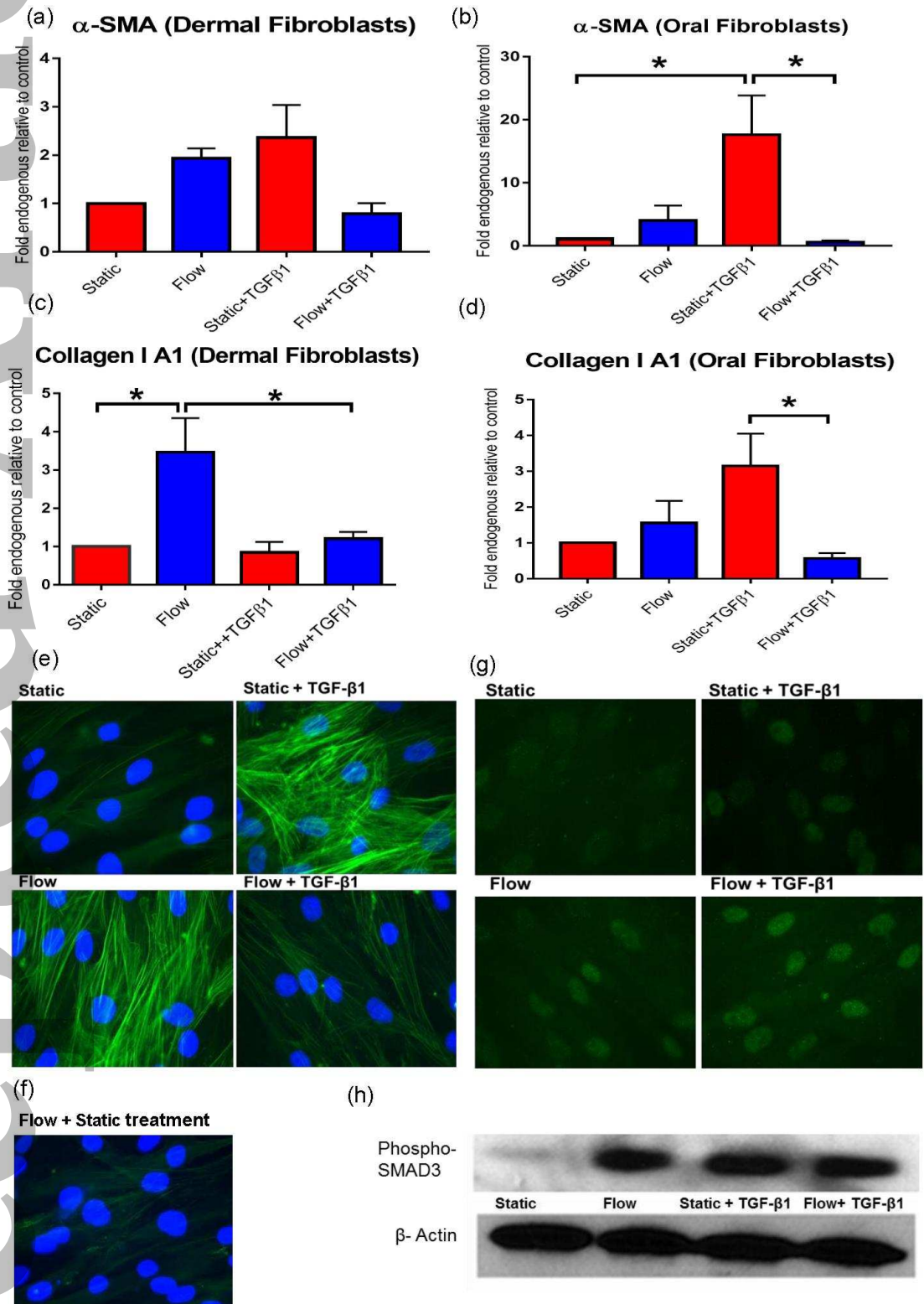
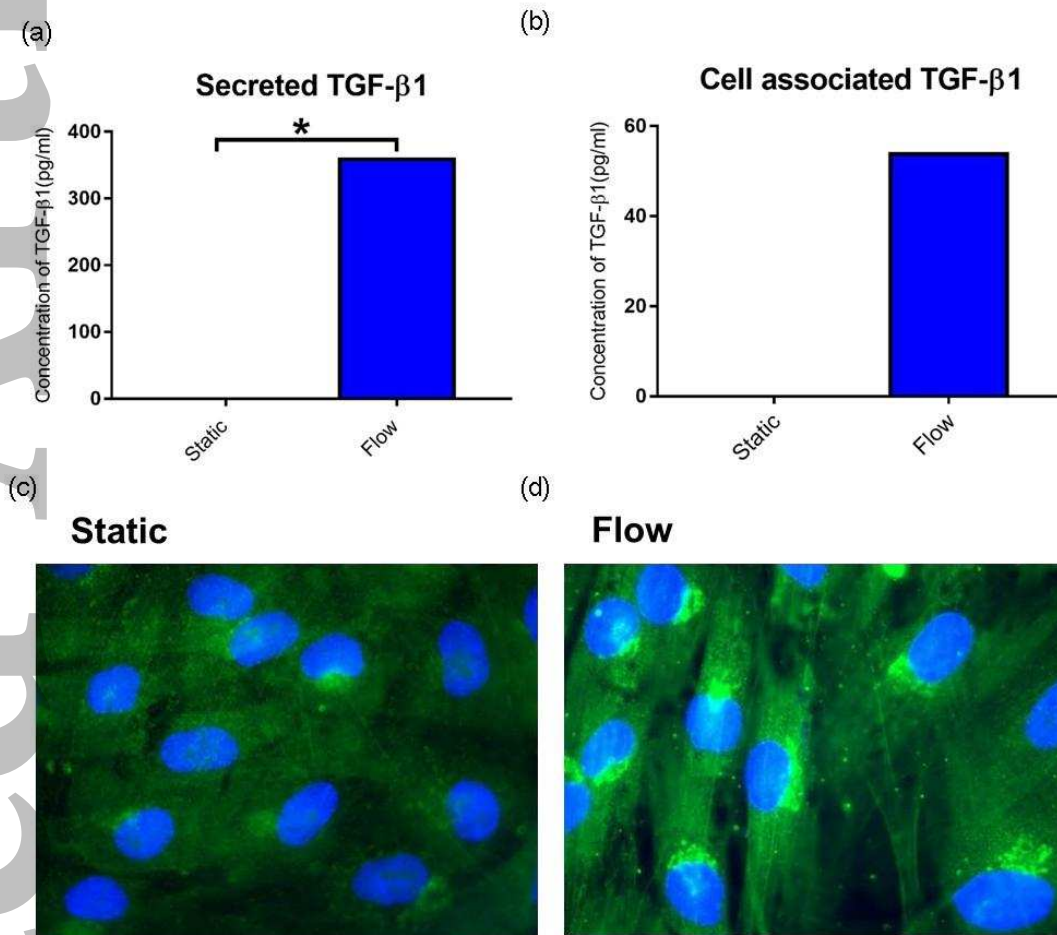
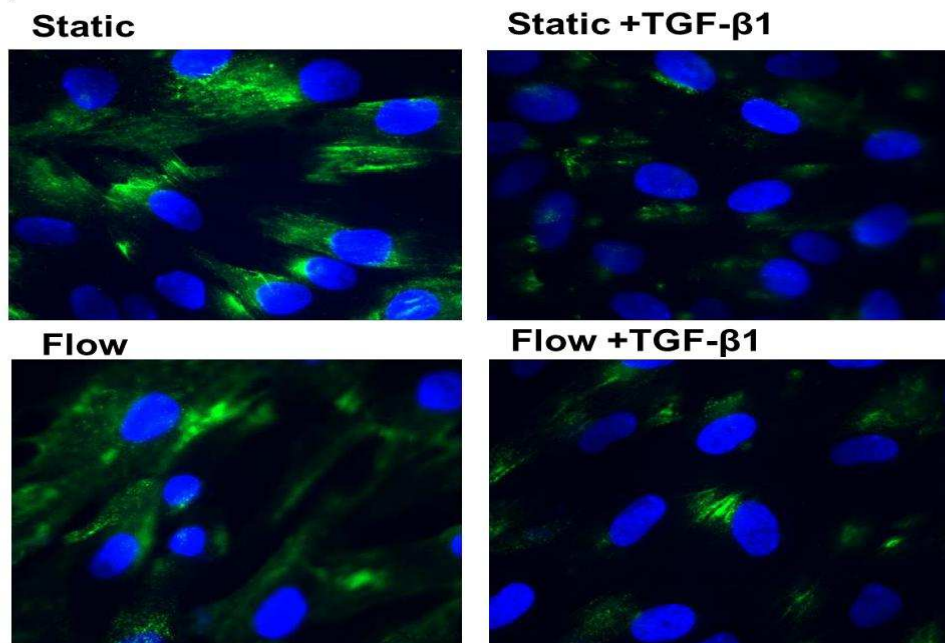


Figure 3:



**Figure 4:**

(a)



(b)

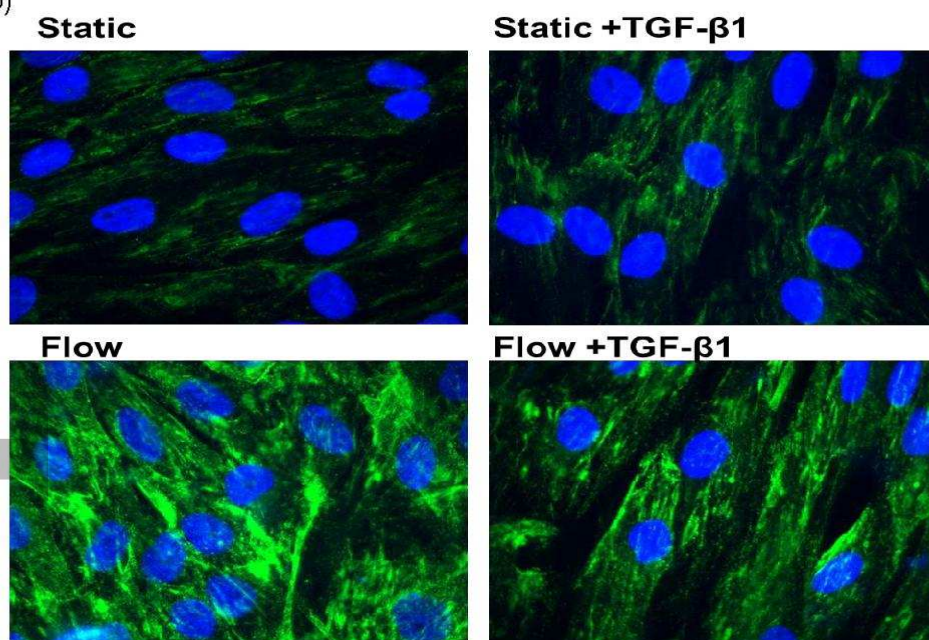
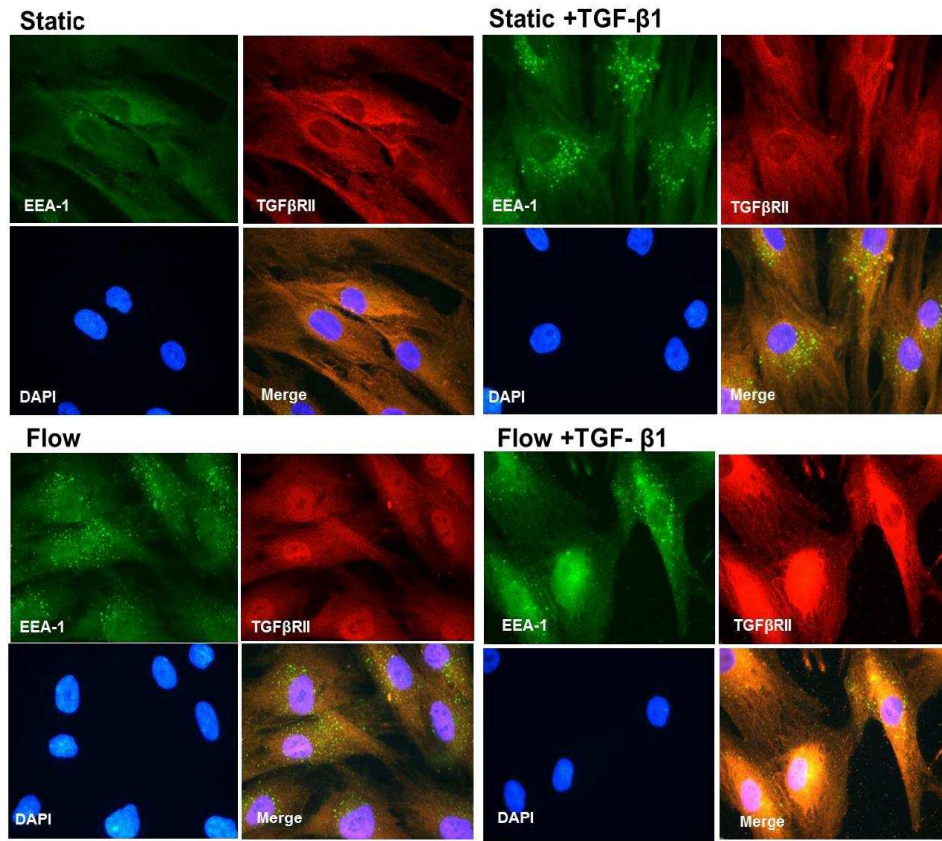
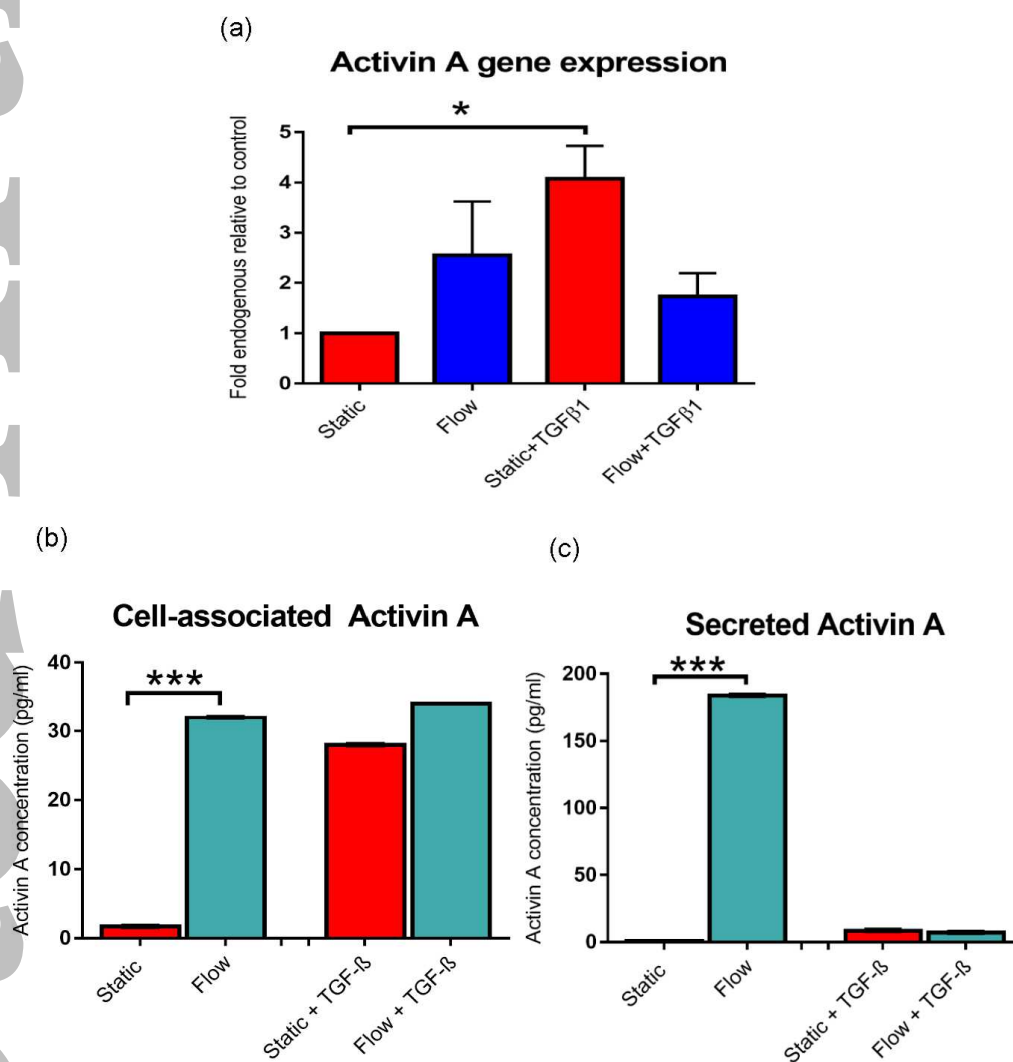


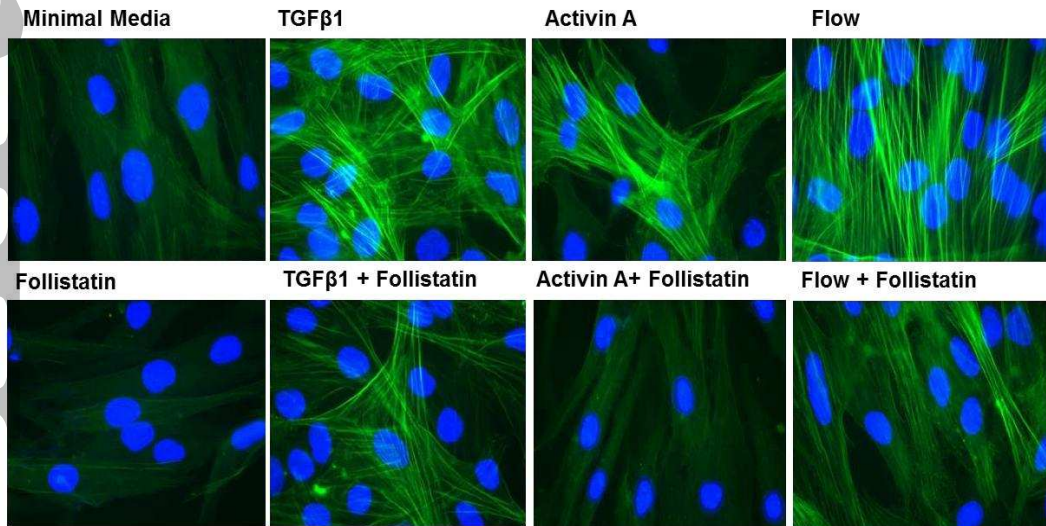
Figure 5:



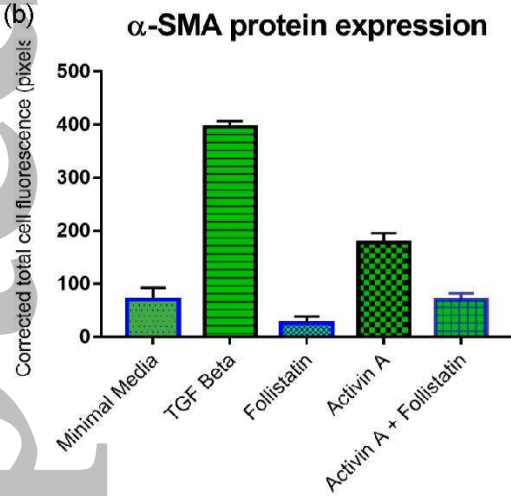
**Figure 6:**

**Figure 7:**

(a)



(b)



(c)

